Biophysical Characterization of Copolymer-Protected Gene Vectors

ARTICLE *in* BIOMACROMOLECULES · JULY 2010

Impact Factor: 5.75 · DOI: 10.1021/bm1002569 · Source: PubMed

Published in final edited form as:
Biomacromolecules. 2010 July 12; 11(7): 1802–1809. doi:10.1021/bm1002569.

Biophysical Characterization of Copolymer-Protected Gene Vectors (COPROGs)

Daniel Hönig[1], **Jason DeRouchey**[2,*], **Ralf Jungmann**[3], **Christian Koch**[4], **Christian Plank**[4], and **Joachim O. Rädler**[1,*]

[1]Ludwig-Maximilians-Universität, Soft Condensed Matter Group, Geschwister-Scholl-Platz 1, 80539 Munich, Germany

[2]Program of Physical Biology, Laboratory of Physical and Structural Biology, National Institute of Child Health and Human Development, National Institutes of Health, Bethesda, Maryland 20892

[3]Technische Universität München, Physics of Biomolecular Systems and Bionanotechnology, James-Franck-Str. 1, 85748 Garching

[4]Institute of Experimental Oncology, Technische Universität München, Ismaninger Str. 22, 81675 Munich, Germany

Abstract

A copolymer-protected gene vector (COPROG) is a three component gene delivery system consisting of a preformed DNA and branched polyethylenimine (bPEI) complex subsequently modified by the addition of a copolymer (P6YE5C) incorporating both poly(ethylene glycol) (PEG) and anionic peptides. Using fluorescence correlation spectroscopy (FCS) and atomic force microscopy (AFM), we characterized and compared the self-assembly of bPEI/DNA particles and COPROG complexes. In low salt buffer, both bPEI/DNA and COPROG formulations form stable nanoparticles with hydrodynamic radii between 60–120 nm. COPROG particles, as compared to bPEI/DNA, show greatly improved particle stability to both physiological salt as well as low pH conditions. Binding stoichiometry of the three-component COPROG system was investigated by dual-color fluorescence cross-correlation spectroscopy (FCCS). It was found that a significant fraction of P6YE5C copolymer aggregates with excess bPEI forming bPEI/P6YE5C “ghost complexes” with no DNA inside. The ratio of ghost particles to COPROG complexes is about 4:1. In addition we find a large fraction of excess P6YE5C copolymer, which remains unbound in solution. We observe a 2–4 fold enhanced reporter gene expression with COPROG formulations at various equivalents as compared to bPEI-DNA alone. We believe that both complex stabilization as well as the capture of excess bPEI into ghost particles induced by the copolymer is responsible for the improvement in gene expression.

Keywords

NONVIRAL GENE DELIVERY; PEI; PROTECTIVE COPOLYMERS; STERIC STABILIZATION; PEG-COATING; TRANSFECTION; EXPRESSION; DIFFUSION; FLUORESCENCE CORRELATION SPECTROSCOPY; FCS

deroucja@mail.nih.gov or joachim.raedler@physik.uni-muenchen.de.

Introduction

The delivery of nucleic acid into cells *in vitro* and *in vivo* is a critical technique for the study of genes and development of potential gene therapies. To fully utilize this potential, safer and more efficient vectors for delivery of genes are required. Current nucleic acid delivery falls into two major categories, viral and non-viral. In non-viral gene delivery, cationic lipids or polymers are used to both protect nucleic acids from degradation and facilitate entry into the target cells. The resulting complexes self-assemble via electrostatic interactions to form stable aggregates. Several recent reviews have discussed the promise of lipid-DNA (lipoplex) and polycation-DNA complexes (polyplexes)1⁻11 as potential therapeutics including recent efforts to incorporate bioresponsive chemistries for increased effectiveness.12, 13

Successful gene transfer requires sufficient stability of DNA during the extracellular delivery phase, transportation through cell membranes and cytoplasm, and eventual disassembly and nuclear delivery. A molecular architecture that achieves all the requirements will most likely consist of a virus-like layered structure incorporating several components. Though nonviral gene vectors can be efficient *in vitro* and *in vivo*, their uncontrolled and often undefined interactions under physiological conditions still represent a major obstacle to their use in gene therapy. In particular, it has been shown that nonviral gene vectors or their constituents interact strongly with negatively charged serum proteins and other blood components. Such opsonization alters the physico-chemical characteristics of vectors, may interfere with vector targeting and is of concern if vectors are to be applied in humans. Consequently, one major objective in nonviral vector development is to devise vectors which are inert in the *in vivo* environment during the delivery phase.

Poly(ethylene glycol) (PEG) has often been used to confer to these drug carriers the desired stability during the extracellular delivery phase. The incorporation of PEG to lipo- or polyplexes has proved effective in reducing undesired effects such as immune response, unspecific interactions, and degradation. PEGylation can be implemented by using PEGylated components in the initial complex formation. Alternatively, PEG shielding can be applied to preformed complexes in a secondary processing step by using either electrostatic self-assembly or chemical grafting.14⁻18 While PEGylation is a necessity to improve extracellular stability and circulation half-life, it often decreases the transfection efficiency due to reduced specificity and inhibited cell association and uptake. Incorporating receptor targeting or using bioresponsive linkers to release PEG have proven useful to overcome these intracellular barriers to efficient delivery.12, 13, 19, 20

Previous work with a copolymer-protected gene vector (COPROG) consisting of branched polyethylenimine (bPEI)/DNA polyplex subsequently shielded with a copolymer consisting of both PEG and anionic peptides (P6YE5C) showed the presence of the copolymer provides steric stabilization, protection from opsonization and allows freeze drying of the vector with little loss of activity.21⁻23 COPROG particles have shown to be effective gene delivery vectors with decreased cellular toxicity without impairing gene transfer. The decreased toxicity of COPROG is likely a result of the removal of unbound polycation by the excess anionic copolymer emphasizing the potential role of binding stoichiometry in three component complexes. Likely due to their stabilizing and opsonization-inhibiting properties, COPROG has proven advantageous in promoting the tranfection capacity of polyplex-loaded sponges upon subcutaneous implantation, and when co-lyophilized with fibrinogen are a simple means to achieve an injectable fibrin gene-activated matrix.22, 23 In this paper, we focus on a comparative biophysical characterization of bPEI/DNA and COPROG complexes with fluorescence correlation spectroscopy (FCS) and atomic force microscopy (AFM). bPEI/DNA and COPROG particle stability to physiological salt and pH

conditions is investigated. We determine the stoichiometry in the COPROG system, in particular the amount of excess bPEI and excess copolymer. Using dual-color fluorescence cross-correlation spectroscopy (FCCS), we also show that the excess bPEI is complexed into bPEI-copolymer ghost particles deficient in DNA. Lastly the COPROG transfection efficiency is compared to bPEI/DNA in NIH-3T3 mouse fibroblasts cells.

MATERIALS AND METHODS

Materials

4.7 kbp pEGFP-N1 and pMetLuc-Control plasmid DNAs were purchased from Clontech (Mountain View, USA), and branched polyethylenimine (25 kDa) from Sigma (Deisenhofen, Germany). The synthesis of the protective copolymer P6YE5C with a backbone consisting of strictly alternating units of PEG-6000 and branched peptide YE5C (sequence: $(Ac\text{-}YE_5)_2K\text{-}ahx\text{-}C$; ahx = 6-aminohexanoic acid) was described in detail previously.21, 22 NIH-3T3 mouse fibroblasts and Metridia luciferase assay (Clontech, USA) were used for transfection efficiency experiments.

Preparation of PEI/DNA and COPROG Polyplexes

For fluorescence correlation spectroscopy (FCS) measurements, 1 μg plasmid DNA and 1.044 μg bPEI were mixed in water. This ratio is equivalent to a nitrogen to phosphate (N/P) charge ratio of 8 which is used in all our experiments except as explicitly indicated. Upon mixing, plasmid DNA and branched polyethylenimine (bPEI) were vortexed and incubated at room temperature for 20 min. These samples were subsequently diluted in water to a final volume of 250 μl. The ternary COPROG complex is prepared similarly. bPEI/DNA is mixed at N/P 8 to form a precomplex. After 20 min, the protective copolymer P6YE5C was added at three charge equivalents, with respect to DNA charge, to the resulting bPEI/DNA precomplex. For FCS experiments, DNA was labeled with Cy5 (Mirus Bio, Madison, USA). bPEI and P6YE5C were labeled with Alexa488 and Alexa633 respectively (Invitrogen, Karlsruhe, Germany). For AFM experiments, bPEI/DNA and COPROG polyplexes were formed as described above using 330 ng of DNA in 10μl TAE-buffer.

Fluorescence Correlation Spectroscopy (FCS) and Dual Color Cross-Correlation Spectroscopy (FCCS) Setup

We used a commercially available Carl Zeiss ConfoCor2 with an Axiovert 200M microscope (Carl Zeiss, Jena, Germany), with Zeiss C-Apochromat (63× NA 1.2) water immersion objective. The illumination source was a 488 nm line of the Argon-Ion laser for Alexa 488 with emission passed through a 505–550 nm band pass filter before detection. For Alexa 633 and Cy5, samples were run with a HeNe laser (633 nm, 5 mW) and emission was passed through a 650 nm long pass before detection. Fluorescent light was recorded by avalanche photo diodes (APDs) in each channel. All FCS/FCCS measurements were performed in NUNC LabTek 8-well microscopy chambers with a final sample volume of 250 μL. Determination of the focal volume was established via calibration against an aqueous solution of Alexa488 ($D = 316\ \mu m^2 s^{-1}$) for the green channel and with Cy5 ($D = 250\ \mu m^2 s^{-1}$) for the red channel. FCS results are an average of 10 measurements made for each sample with sampling times of 30s. All measurements were performed at room temperature and in distilled water.

FCS/FCCS Data Analysis

Since, the principles of FCS and dual-color fluorescence cross-correlation (FCCS) in confocal setups have been previously described in a number of reviews, here we will give only a brief overview.24–30 In FCS, the raw signal is the time-dependent fluorescence

intensity emitted by labeled objects diffusing through a highly focused illuminated volume (~1 fL). The size of the effective illumination volume is fixed by the confocal detection optics and the excitation profile of the focused laser beam and characterized by measurements against a standard of a known diffusion constant. As labeled particles diffuse through the detection volume, a signal is generated with fluctuations around a mean value. For identical fluorescent particles undergoing ideal Brownian diffusion, dynamic information can be determined from the intensity fluctuations by means of a time autocorrelation given by

$$G_{ideal}(\tau)=1+\frac{1}{N}\bullet\frac{1}{1+\frac{\tau}{\tau_D}}\bullet\frac{1}{\sqrt{1+\frac{\tau}{S^2\tau_D}}} \quad (1)$$

Here, N denotes the number of particles per effective volume and the structure parameter S = ω_z/ω_x is the ratio of the axial to radial dimensions of the focused excitation beam as determined by calibration measurements (S was approximately 5–6 in our experiments). The diffusion time τ_D is related to the translational diffusion coefficient D by the simple relationship $\tau_D = \omega_x^2/4D$. In general, one also sees correlations arising from intramolecular dynamic processes involving dark states, such as triplet states, or from experimental afterpulsing. Assuming that these processes are well separated in the time domain, the full autocorrelation function can then be written as

$$G(\tau)=G_{ideal}(\tau)\times g_{tr}(\tau) \quad (2)$$

where $g_{tr}(\tau) = [1+\exp(-\tau/\tau_T)]T/(1-T)$ is the autocorrelation function related with dark fractions T and characteristic flickering times τ_T typically observed to be of the order of 2 μs and well separated from the time scales of interest in these experiments. In dilute solution, the autocorrelation can thus normalized by

$$G_{norm}(\tau)=\frac{G(\tau)-1}{G(0)-1} \quad (3)$$

For spherical particles with hydrodynamic radius RH smaller than the detection volume ($R_H \ll \omega_x$), the hydrodynamic radius, R_H, can be calculated from the Stokes-Einstein relation

$$R_H=\frac{k_bT}{6\pi\eta D_t} \quad (4)$$

where η is the solvent viscosity, k_b is the Boltzmann constant, and T is the temperature. In the case of multicomponent systems the correlation function is given as a sum of weighted correlation

$$G(\tau)=\sum_{i=1}^{M}q_i^2N_i^2G_i(\tau)\Big/\left[\sum_{i=1}^{M}q_iN_i\right]^2 \quad (5)$$

where N_i and $G_i(\tau)$ are the mean number and autocorrelation functions due to the the diffusion of the *i*th species in the focal volume. q_i designates the ratio of the fluorescence yield of the *i*th species to that of species 1, taken as reference.

Dual-color fluorescence cross-correlation spectroscopy (FCCS) exploits the temporal fluorescence fluctuations coming from two differently labeled molecules. In FCCS, the fluorescence emission signals from the two dyes are separately detected and, in addition to the autocorrelation, the cross-correlation function is calculated to give information regarding the dynamics of the dual-labeled molecules. Here, the autocorrelation of a single channel can be calculated as above with the cross-correlation between two channels, for example red and green, calculated simply as

$$G_{cross}(t)=\frac{\left\langle F_{green}(t)\bullet F_{red}(t+\tau)\right\rangle}{\left\langle F_{green}(t)\right\rangle\langle F_{red}(t)\rangle} \tag{6}$$

Importantly, the cross-correlation can give not only the diffusion properties of double-labeled (red and green) particles, but the cross-correlation amplitude is directly proportional to the concentration of double-labeled species

$$\left\langle C_{gr}\right\rangle=\frac{G_{gr}(0)}{V_{eff}G_r(0)G_g(0)} \tag{7}$$

Where Veff is the effective detection volume for the dual color experiment as determined by the axial and radial dimensions of the two beams and defined as

$$V_{\text{eff}}=\frac{\pi^{3/2}\left(\omega_{x,g}^2+\omega_{x,r}^2\right)\left(\omega_{z,g}^2+\omega_{z,r}^2\right)^{1/2}}{2^{3/2}} \tag{8}$$

Atomic Force Microscopy

Samples were imaged in tapping mode using a Multimode V AFM with Nanoscope V controller and E-scanner (Veeco Instruments, Santa Barbara, USA). Imaging was performed in distilled water using DNP-S oxide-sharpened silicon nitride cantilevers (Veeco Probes, Camarillo, USA) at resonance frequencies between 7–9 kHz. Ultrapure water, used throughout this study, was provided by a Barnstead EASYPure II system (Werner GmbH, Germany) coupled to an ion exchange unit (Werner GmbH). For bPEI/DNA complexes, 5 μl of the sample solution was deposited onto a freshly cleaved mica surface (Plano, Dresden, Germany) and rinsed with ultrapure water after incubating for 30 s. For COPROG imaging, a freshly cleaved mica surface was pretreated with 20 μl of TAE/Mg^{2+} buffer solution (1× TAE, 12.5 mM magnesium acetate (pH 8.3) buffer solution).31–33 After 30 s, the mica surface was dried using a gentle stream of N_2 and 5 μl of the sample solution was placed onto the mica surface. After another 30 sec, the adsorbed samples were washed with an additional 30 μl of ultrapure water.

After engaging the surface, imaging parameters were optimized for best image quality while maintaining the highest possible setpoint to minimize damage to the samples. Images were post processed by subtracting a 1st order polynomial from each scan line. Drive amplitudes were approximately 0.1 V, integral gains approximately 2, proportional gains approximately 4. Image analyzing for lateral size distribution determination of the COPROGs was performed with NI Vision toolbox in NI LabView (National Instruments, Austin, USA). Briefly, the AFM image is first subjected to a locally adaptive thresholding algorithm for binarization and subsequently a circular pattern detection algorithm is used to determine circular shaped features in the binary image, thus omitting particles distorted by AFM

imaging artifacts such as well-known tapping mode “tails”.34 MATLAB (The MathWorks, Natick, USA) was used to create a histogram plot of the extracted diameters with a bin size of 31.3 nm and subsequent fitting to a Gaussian distribution.

Cell culture and transfections

Cell transfection experiments were made in NIH-3T3 mouse fibroblasts (DSMZ No. 45526). NIH-3T3 cells were cultured at 37°C and in an atmosphere of 5% CO_2 in Dulbecco’s Modified Eagle Medium (Invitrogen, Karlsruhe, Germany) supplemented with 10 % fetal calf serum 100 units / ml penicillin 100 µg / ml streptomycin and 2 mM glutamine. One day before transfection, cells were split and seeded in a 96-well plate at a density 5,000 per well. COPROGs were prepared at a final DNA (pMetLuc-Control) concentration of 20 µg/mL in water as described above. Immediately before transfection, which was carried out in triplicates, the supernatants in the 96-well cell culture plate were replaced with 150 µl of fresh medium. 50 µl aliquots of COPROGs (corresponding to 1 µg DNA) were added. At 24, 48 and 72 hours the medium was changed completely and 200 µl fresh medium was added to the wells. The pMetLuc2-Control plasmid encodes Metridia luciferase which is secreted from transfected cells. For the detection of Metridia luciferase, 50 µl of the cell culture media was transferred into white 96-well plates and mixed with 20 µl of a 50 µM coelenterazine solution in PBS. The luciferase activity produces blue light at λ= 480nm which was detected by a Wallac Victor 2 Multi Label Counter (Perkin Elmer, Waltham, USA).

RESULTS AND DISCUSSIONS

COPROG formation

Copolymer-protected gene vectors (COPROGs) were prepared as described previously and as schematically represented in Figure 1.21, 22 COPROG gene vectors are ternary complexes self-assembled via electrostatic interactions in a two-step protocol to form PEG shielded gene vectors with increased particle stability. First, plasmid DNA is mixed together with a 25 kDa branched polyethylenimine (bPEI) cationic polymer at a nitrogen to phosphate (N/P) charge ratio of 8. bPEI/DNA at high N/P ratios form small stable nanoparticles with a positive surface charge as determined by zeta-potential measurements. These charged colloidal particles form a COPROG precomplex. P6YE5C, a copolymer incorporating both negatively charged peptide sequences and the sterically stabilizing uncharged polymer poly(ethylene glycol) (PEG), is subsequently added at three charge equivalents, with respect to DNA phosphates, to form the final COPROG nanoparticles. As described previously, the COPROG complexes have a zeta potential close to zero.21

FCS and AFM measurements of bPEI/DNA and COPROG Complexes

FCS measurements were first performed on cy5-labeled pEGFP-N1 plasmid DNA (4.7 kbp) in distilled water at room temperature. The resulting autocorrelation curve was normalized and is shown as the solid line in Figure 2. The same Cy-5 labeled plasmid was subsequently used in the preparation of bPEI/DNA (N/P 8) and COPROG polyplexes (dashed and dotted lines, respectively) to compare the resulting complexes diffusion properties in water. Data was acquired after 20 min of incubation at room temperature. All autocorrelation curves can be fit using equation 3 and are well described with a single mean dwell time, τ_D. The hydrodynamic radius (R_H) can be determined from equation 4 as $R_H = 70 \pm 10$ nm for both bPEI/DNA and COPROG nanoparticles under these low ionic strength conditions. Uncondensed plasmid diffuses with a $\tau_D \sim 1$ ms corresponding to an apparent hydrodynamic radius of 220 nm.

In the presence of NaCl, the sizes and the polydispersities of the bPEI/DNA and COPROG complexes differ dramatically. Figure 3 shows the FCS autocorrelation curves for bPEI/DNA and COPROG particles in 150 mM NaCl solutions, comparable to physiological salt conditions. The increased salt stability of COPROG is clearly visible. FCS autocorrelation curves of bPEI/DNA in NaCl shows clear signs of significant aggregation. Since both bPEI/DNA and COPROG samples were made with the same initial DNA concentration, the sharp increase in the plateau region of the bPEI/DNA autocorrelation curve indicates a significant decrease in the measured number of particles N. In addition, τ_D for bPEI/DNA shifts to hundreds of ms corresponding to an average hydrodynamic radius of several microns. In contrast, the addition of P6YE5C copolymer to form the COPROG complex has greatly increased the particle stability to salt. COPROG autocorrelation curves look nearly identical to low ionic salt conditions and maintain an $R_H \sim 70$ nm. These results correspond well with previous dynamic light scattering measurements.21 Maintaining size stability at physiological salt concentrations is critical for systemic delivery of the gene vector.

The effect of stoichiometry of the COPROG formulation on salt stability was also investigated by FCS. Figure 4 shows the hydrodynamic radii, R_H of COPROG complexes, made with a constant three charge equivalents of P6YE5C, but with various N/P ratios as a function of NaCl salt concentration. Complexes are observed to stay monodisperse and stable in size with R_H ranging from 60–110 nm for all three N/P ratios up to physiological salt concentrations (~150 mM NaCl). This data suggests improved particle stability for COPROG formulations for systemic delivery with higher N/P ratios giving smaller and more stable complexes at low salt. At significantly high salt concentrations, the COPROG shielding by P6YE5C is insufficient to suppress aggregation and micron sized aggregates are observed.

Previous work has suggested that polyethylenimine enhances transgene delivery through a “proton sponge” effect where the buffering capacity of PEI leads to endosomal chloride ion accumulation creating an osmotic swelling and eventual rupture of endosomes.35–37 This enhanced endosomal escape presumably is a major contributor to the observed higher transfection efficiencies for PEI compared to non-buffering polyamines such as polylysine. To compare pH effects on bPEI and COPROG polyplexes, we investigated both the size and number of the complexes by FCS.

Figure 5 shows the hydrodynamic radii, RH and total number of particles, N for bPEI/DNA and COPROG over a pH range of 5 to 7.4. For all systems, N/P charge ratio for the bPEI amines to DNA phosphates was fixed to 8 with a constant DNA concentration of 4 μg/mL. All COPROG complexes were mixed with a fixed three charge equivalent of P6YE5C. Data shown was collected using Alexa488 labeled bPEI instead of Cy5-labeled plasmid as was used for the previous figures. The resulting ~75–110 nm hydrodynamic radii at pH ~ 7 for bPEI and COPROG complexes are fairly consistent with prior experiments using the labeled plasmid showing minimal effects from the labeling process. COPROG particles show significantly increased stability to pH and maintain both the size and number of particles over the full range. bPEI polyplexes, in contrast, show a distinct jump in both R_H and N at pH below 6.5. The large increase in particle size at low pH is consistent with significant aggregation of the bPEI/DNA complexes at low pH. However, we also observe an increase in the total number of particles suggesting the release of bound Alexa488-bPEI at low pH presumably due to a charging effect of the bPEI amines. The exact nature of the pH release of bound bPEI or how P6YE5C alters the bPEI buffering capacity is currently not fully understood.

Since the size of transfection particles is a critical parameter influencing biological properties, complexes were also analyzed using AFM. Figure 6 shows height and amplitude

images (A and B, respectively) for bPEI/DNA complexes (N/P 8) on untreated freshly cleaved mica surfaces. The presence of excess bPEI and the positive zeta potential of the resulting bPEI/DNA polyplexes compensate for the negative charge of the freshly exposed mica surface and the complexes are observed to adhere consistently to the bare mica. Particles were observed to be highly condensed and of approximately spherical character with diameters of approximately 100 nm. To improve the adhesion of COPROG particles, where both the complex zeta potential becomes close to zero or negative and the amount of free bPEI is greatly reduced due to the presence of the negative P6YE5C copolymer, the cleaved mica surface was pretreated with a TAE/Mg^{2+} buffer. Buffer solutions containing divalent cations like Mg^{2+} are commonly used in AFM studies on mica surfaces to attach negatively charged polymers such as DNA. Figure 6 C/D show height and amplitude images for COPROG complexes and show the resulting dimensions are very similar to the bPEI/DNA polyplexes of Figure 6 A/B.

For a rough size estimation of the COPROG complexes we imaged a 10 × 10 μm^2 area and determined the apparent size distribution of the particles as described in the materials and methods section. A Gaussian fit to the size distribution gives a mean diameter of 94.2 ± 23.5 nm. Despite potential errors to lateral size determination, such as the effect of tip broadening or possible changes in the native conformational state of the COPROGs due to interactions with charged surfaces, the measured apparent diameters are in good agreement with our FCS measurements and show a narrow distribution.

FCCS of COPROG Complexes

Dual-color fluorescence cross-correlation spectroscopy (FCCS) was used to investigate the binding stoichiometry of the COPROG gene vectors. For the cross-correlation experiments, Alexa488 labeled bPEI (green channel) and Alexa633 P6YE5C (red channel) were used. Single color autocorrelation analysis was first used to determine the diffusion coefficients of bPEI and P6YE5C independently. Diffusion coefficients D of 2.6×10^{-10} m^2s^{-1} for Alexa488-bPEI and 6.0×10^{-11} m^2s^{-1} for the P6YE5C copolymer were obtained and are tabulated in Table 1. Dual-color FCCS measurements were performed on COPROGs made with three charge equivalents and the results are shown in Figure 7 and Tables 2 and 3. For all autocorrelation curves shown in Figure 7, the data was best fit by a two component model and plotted as a solid line. Focusing first on the fast fraction ρred1 of the red channel, the measured dwell time of 0.12 ms corresponds well to the previously measured autocorrelation of unbound P6YE5C. In contrast, the fast fraction ρgreen,1 of the green channel measured a dwell time τ_D = 0.155 ms (D ~ 5.0×10^{-11} m^2s^{-1}), which exceeds the dwell time measured for free bPEI. It appears that this fast diffusion time corresponds to the autocorrelation of bPEI complexed with P6YE5C without incorporation of DNA. Indeed preparation of such “ghost complexes” in binary PEI-P6YE5C mixtures exhibit a diffusion coefficient of D ~ 5.0×10^{-11} m^2s^{-1} in agreement with the diffusion time measured for the fast component (data not shown). The slow fraction in all three correlation curves in Figure 5 ($\rho_{red,2}$, $\rho_{green,\ 2}$, $\rho_{cross,\ 2}$) corresponds to the COPROG complexes. Note that the apparent diffusion time of the COPROG complexes in the cross-correlation curve is slightly larger than in both, the red and green channel autocorrelation curves due to incomplete detection volume overlap.28 Estimating the diffusion coefficient of COPROG particles from the autocorrelations (τ_D ~ 3.3 ms), we get D_{COPROG} ~ 2.5×10^{-12} m^2s^{-1} in agreement with the data shown in Figure 2.

A fully quantitative analysis of the stoichiometric ratios in the complexes requires knowledge of the molecular brightness, q, of the various fluorescent species (see equation 5). Clamme et al. measured q = 3.2 for PEI-DNA complexes indicating strong quenching of the chromophore TRITC in the complexes.38 Assuming the same quenching factor for the P6YE5C red fluorescence, the ratio of the amplitude 93.6% P6-ghost particles and 6.4% for

the COPROG complexes would suggest an actual P6YE5C content estimated at only a couple percent in the COPROG particles. While not truly quantitative, our measurements clearly suggest an abundance of P6YE5C molecules either free in solution or complexed in bPEI/P6YE5C ghost particles. The fact that the diffusion time of the fast fraction of the green channel (bPEI) coincides with the diffusion time of bPEI/P6YE5C ghost particles indicates complete binding of the bPEI by P6YE5C in the COPROG formulation. The percent concentration in the cross-correlation is also in reasonable agreement with the green channel analysis suggesting that there is no free bPEI left in solution.

Previous estimates of stoichiometry for bPEI/DNA polyplex particles have been reported in the literature. Two photon fluorescence correlation spectroscopy measurements by Clamme et al.38 estimated ~86% of the bPEI was free for N/P charge ratios of 10. Boeckle et al.39 used size exclusion chromatography to remove unbound bPEI resulting in an estimate of N/P ~2.5 to achieve particle neutrality suggesting ~1/3 of the bPEI is incorporated into the bPEI/DNA particle at N/P 8. Surprisingly, from our FCCS measurements ρ_{green} concentrations, we estimate approximately 25% of the bPEI is complexed to P6YE5C while ~75% is incorporated into the COPROG complex. Hence a total of ~23.4% of the P6YE5C copolymer is complexed with bPEI in the form of bPEI-P6YE5C “ghost particles” that contain no DNA. Presumably, the addition of the P6YE5C copolymer induces the additional binding of a significant fraction of the free bPEI into the final COPROG complex. This finding is further confirmed by the cross-correlation function, which exhibits about 82.2% of the bPEI/P6YE5C being bound to the large COPROG particles, while ~17.8% are bPEI/P6YE5C ghost particles. More studies are needed to fully clarify the mechanism and exact stoichiometry resulting from the sequential addition in tertiary complexes.

Comparative Transfection Efficiency Studies of bPEI/DNA and COPROG

Transfections were carried out with adherent NIH-3T3 mouse fibroblasts cells in serum-containing medium. The comparative transfection efficiencies of COPROGs, as a function of charge equivalents of the protective copolymer P6YE5C used during complex formation are shown in Figure 8. For all measurements, the DNA and bPEI ratio and the DNA dose per well were kept constant. Transfection efficiencies were measured after 24, 48 and 72 hours with a Metridias Luciferase assay. Maximum gene expression was observed at 48 hours for all COPROG and bPEI samples. The COPROG stoichiometry of the polycation–DNA core turns out to be important parameter governing transfection efficiency. In good agreement with previous observations, 21 we observe a 2–4 fold enhanced reporter gene expression with increasing amounts of P6YE5C compared to “naked” bPEI-DNA. The DNA dose used in this experiment is rather high (1 μg DNA per well) such that naked bPEI-DNA caused strong toxicity which was significantly reduced with COPROGs. Our findings with FCS measurements confirm previous results which show that 60–80% of branched or linear PEI in PEI polyplexes are in fact not associated with the DNA component but are rather free in solution.38⁻41 On the other hand, it is known that PEI polyplexes where excess PEI has been removed are considerably less toxic than their parent complexes but are less efficient in gene delivery.39⁻41 Boeckle et al have shown that the lost gene transfer efficiency can be fully recovered when cells that have been transfected with purified PEI polyplexes are complemented with free PEI up to 4 hours after transfection. Kichler et al. have shown that part of the coding DNA in unpurified PEI polyplexes can be replaced with stuffer DNA or even poly(glutamic acid) without losing efficiency in reporter gene expression. Uptake of PEI polyplexes into cells is known to proceed via endocytosis and PEI is known to exert the proton sponge effect in internalized vesicles which ultimately leads to endosome disruption. From the findings described above one can conclude that a certain threshold amount of PEI in internalized vesicles is required in order exert the proton sponge effect and to lead to functional gene delivery. From our findings in FCS measurements we conclude that an

essential role of the protective copolymer P6YE5C for gene delivery in cell culture is capturing excess free PEI, that has been previously shown to be toxic to cells,[39, 42, 43] and thereby transforming it in a less toxic complexed form (i.e. ghost complexes). The binary complex of bPEI/P6YE5C could be co-internalized into cells with the ternary complexes comprising bPEI/DNA/P6YE5C and as a stuffer function in analogy to Kichler's findings may lead to a productive proton sponge effect.

Conclusions

Using fluorescence correlation spectroscopy and atomic force microscopy, we have characterized the self-assembly of bPEI/DNA polyplex nanoparticles and tertiary COPROG complexes in comparison. The complex stability in salt and pH was investigated. FCS/FCCS measurements surprisingly showed that only a minor fraction of the protective copolymer P6YE5C is associated with bPEI-DNA nanoparticles forming the actual COPROG particles. The majority of the protective copolymer P6YE5C complexes with excess bPEI into so-called "ghost particles". This finding might explain the known disopsonizing and protective effect of the copolymer and its enhancing effect in gene delivery. The protective polymer has not only a shielding effect on the PEI-DNA nanoparticle, rather, it also "detoxifies" excess free PEI present in PEI polyplex preparations. Furthermore the ghost particle appears to be productive during the intracellular steps of gene delivery. Hence in general the post-processing of gene-delivery vectors by copolymers may enhance efficiency and deserves further attention.

Acknowledgments

The authors thank F. C. Simmel and the Physics of Biomolecular Systems and Bionanotechnology Laboratory for use of the AFM. Funding by the German Federal Ministry of Education and Research as well as by Nanosystems Initiative Munich is gratefully acknowledged. JOR and CP acknowledge funding through BMBF project 0312019A. JOR also acknowledges a travel fund by the ESF. JD was supported in part by the Intramural Research Program of the Eunice Kennedy Shriver National Institute of Child Health and Human Development, National Institutes of Health. RJ was supported by the Elite Network of Bavaria (IDK-CompInt).

References

1. Dass CR. Journal of Molecular Medicine. 2004; 82(9):579–591. [PubMed: 15221077]
2. Li SD, Huang L. Gene Therapy. 2006; 13(18):1313–1319. [PubMed: 16953249]
3. Neu M, Fischer D, Kissel T. Journal of Gene Medicine. 2005; 7(8):992–1009. [PubMed: 15920783]
4. Wagner E. Pharmaceutical Research. 2004; 21(1):8–14. [PubMed: 14984252]
5. Wagner, E.; Kloeckner, J. Gene delivery using polymer therapeutics. In Polymer Therapeutics I: Polymers as Drugs, Conjugates and Gene Delivery Systems. Vol. Vol. 192. 2006. p. 135-173.
6. Itaka K, Kataoka K. European Journal of Pharmaceutics and Biopharmaceutics. 2009; 71(3):475–483. [PubMed: 18955136]
7. MacLachlan I, Cullis P, Graham RW. Current Opinion in Molecular Therapeutics. 1999; 1(2):252–259. [PubMed: 11715948]
8. Niidome T, Huang L. Gene Therapy. 2002; 9(24):1647–1652. [PubMed: 12457277]
9. Wong SY, Pelet JM, Putnam D. Progress in Polymer Science. 2007; 32(8–9):799–837.
10. Mintzer MA, Simanek EE. Chemical Reviews. 2009; 109(2):259–302. [PubMed: 19053809]
11. Morille M, Passirani C, Vonarbourg A, Clavreul A, Benoit JP. Biomaterials. 2008; 29(24–25):3477–3496. [PubMed: 18499247]
12. Wolff JA, Rozema DB. Molecular Therapy. 2008; 16(1):8–15. [PubMed: 17955026]
13. Yu HJ, Wagner E. Current Opinion in Molecular Therapeutics. 2009; 11(2):165–178. [PubMed: 19330722]
14. Verbaan FJ, Oussoren C, Snel CJ, Crommelin DJA, Hennink WE, Storm G. Journal of Gene Medicine. 2004; 6(1):64–75. [PubMed: 14716678]

15. Fisher KD, Ulbrich K, Subr V, Ward CM, Mautner V, Blakey D, Seymour LW. Gene Therapy. 2000; 7(15):1337–1343. [PubMed: 10918506]
16. Ogris M, Brunner S, Schuller S, Kircheis R, Wagner E. Gene Therapy. 1999; 6(4):595–605. [PubMed: 10476219]
17. DeRouchey J, Schmidt C, Walker GF, Koch C, Plank C, Wagner E, Radler JO. Biomacromolecules. 2008; 9(2):724–732. [PubMed: 18220349]
18. DeRouchey J, Walker GF, Wagner E, Radler JO. Journal of Physical Chemistry B. 2006; 110(10): 4548–4554.
19. Wagner E. Expert Opinion on Biological Therapy. 2007; 7(5):587–593. [PubMed: 17477797]
20. Walker GF, Fella C, Pelisek J, Fahrmeir J, Boeckle S, Ogris M, Wagner E. Molecular Therapy. 2005; 11(3):418–425. [PubMed: 15727938]
21. Finsinger D, Remy JS, Erbacher P, Koch C, Plank C. Gene Therapy. 2000; 7(14):1183–1192. [PubMed: 10918486]
22. Scherer F, Schillinger U, Putz U, Stemberger A, Plank C. Journal of Gene Medicine. 2002; 4(6): 634–643. [PubMed: 12439855]
23. Schillinger U, Wexel G, Hacker C, Kullmer M, Koch C, Gerg M, Vogt S, Ueblacker P, Tischer T, Hensler D, Wilisch J, Aigner J, Walch A, Stemberger A, Plank C. Pharmaceutical Research. 2008; 25(12):2946–2962. [PubMed: 18781379]
24. Eigen M, Rigler R. Proceedings of the National Academy of Sciences of the United States of America. 1994; 91(13):5740–5747. [PubMed: 7517036]
25. Schwille P, MeyerAlmes FJ, Rigler R. Biophysical Journal. 1997; 72(4):1878–1886. [PubMed: 9083691]
26. Hess ST, Huang SH, Heikal AA, Webb WW. Biochemistry. 2002; 41(3):697–705. [PubMed: 11790090]
27. Bacia K, Kim SA, Schwille P. Nature Methods. 2006; 3(2):83–89. [PubMed: 16432516]
28. Bacia K, Schwille P. Nature Protocols. 2007; 2(11):2842–2856.
29. Haustein E, Schwille P. Annual Review of Biophysics and Biomolecular Structure. 2007; 36:151–169.
30. Hwang LC, Wohland T. Cell Biochemistry and Biophysics. 2007; 49(1):1–13. [PubMed: 17873335]
31. Bustamante C, Vesenka J, Tang CL, Rees W, Guthold M, Keller R. Biochemistry. 1992; 31(1):22–26. [PubMed: 1310032]
32. Hansma HG, Vesenka J, Siegerist C, Kelderman G, Morrett H, Sinsheimer RL, Elings V, Bustamante C, Hansma PK. Science. 1992; 256(5060):1180–1184. [PubMed: 1589799]
33. Vesenka J, Guthold M, Tang CL, Keller D, Delaine E, Bustamante C. Ultramicroscopy. 1992; 42:1243–1249. [PubMed: 1413262]
34. Volcke C, Pirotton S, Grandfils C, Humbert C, Thiry PA, Ydens I, Dubois P, Raes M. Journal of Biotechnology. 2006; 125(1):11–21. [PubMed: 16860705]
35. Behr JP. Chimia. 1997; 51(1–2):34–36.
36. Sonawane ND, Szoka FC, Verkman AS. Journal of Biological Chemistry. 2003; 278(45):44826–44831. [PubMed: 12944394]
37. Akinc A, Thomas M, Klibanov AM, Langer R. Journal of Gene Medicine. 2005; 7(5):657–663. [PubMed: 15543529]
38. Clamme JP, Azoulay J, Mely Y. Biophysical Journal. 2003; 84(3):1960–1968. [PubMed: 12609898]
39. Boeckle S, von Gersdorff K, van der Piepen S, Culmsee C, Wagner E, Ogris M. Journal of Gene Medicine. 2004; 6(10):1102–1111. [PubMed: 15386739]
40. Erbacher P, Bettinger T, Brion E, Coll JL, Plank C, Behr JP, Remy JS. Journal of Drug Targeting. 2004; 12(4):223–236. [PubMed: 15506171]
41. Kichler A, Leborgne C, Danos O. Journal of Gene Medicine. 2005; 7(11):1459–1467. [PubMed: 16041686]

42. Moghimi SM, Symonds P, Murray JC, Hunter AC, Debska G, Szewczyk A. Molecular Therapy. 2005; 11(6):990–995. [PubMed: 15922971]

43. Brunot C, Ponsonnet L, Lagneau C, Farge P, Picart C, Grosgogeat B. Biomaterials. 2007; 28(4): 632–640. [PubMed: 17049374]

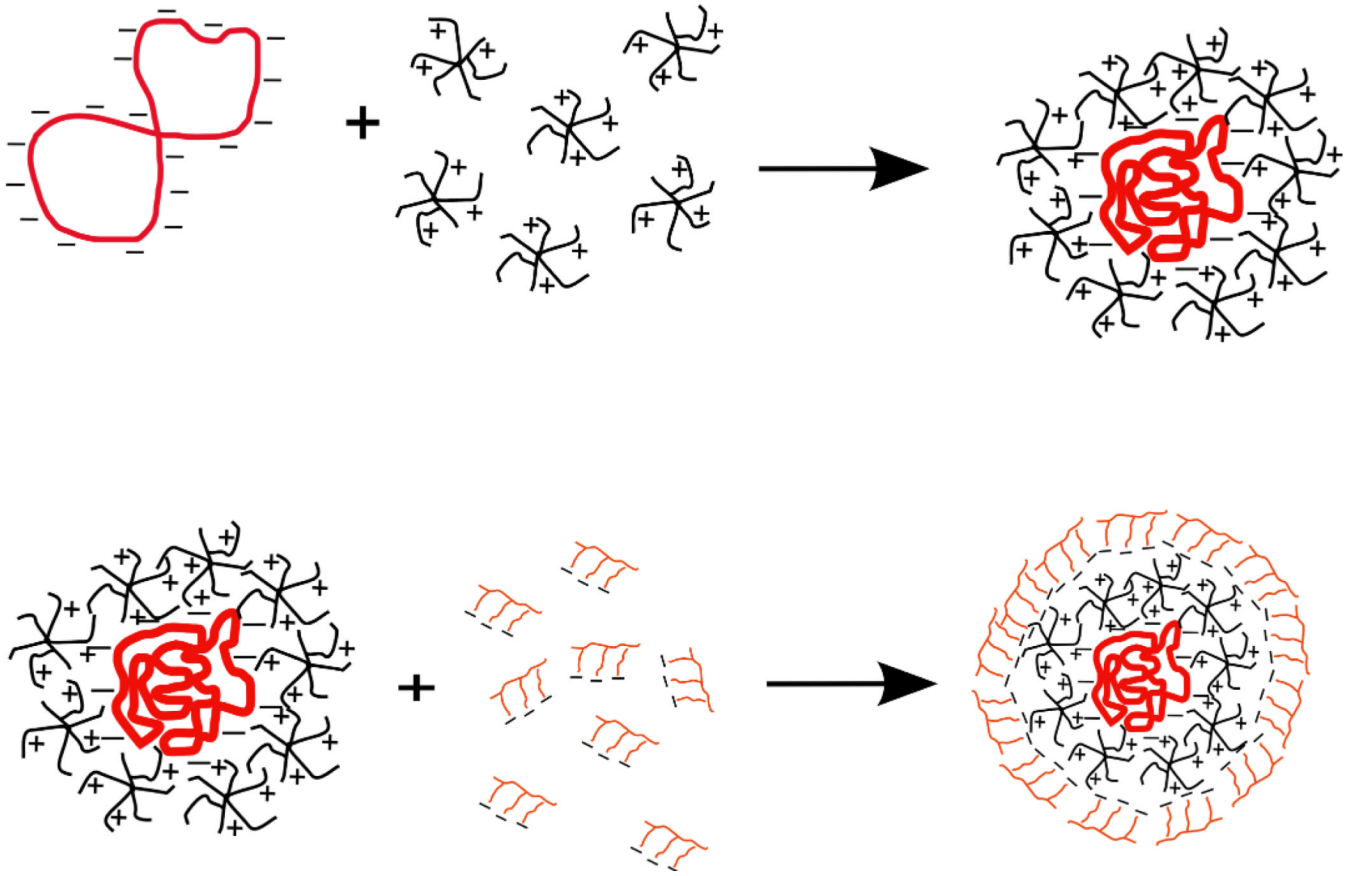

Figure 1.
Schematic drawing of the self-assembly of copolymer protected gene vectors (COPROGs). Plasmid DNA are mixed with 25kDa branched polyethylenimine (N/P = 8) to form a bPEI/DNA precomplex. After incubation, the positively overcharged precomplex is mixed with the negatively charged copolymer P6YE5C. All preparation steps are made in distilled water.

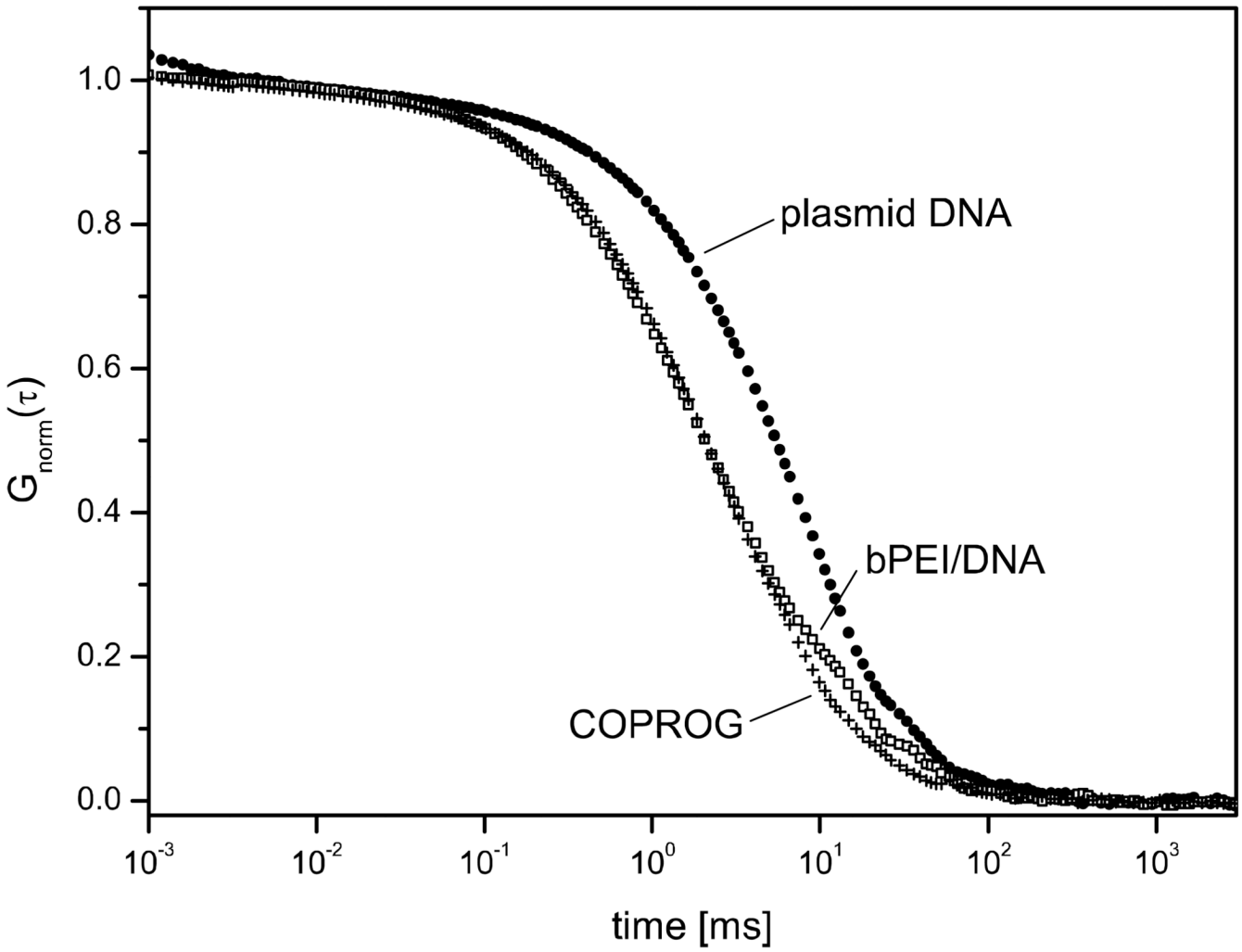

Figure 2.
Normalized FCS autocorrelation curves of plasmid (●), bPEI/DNA (□) and COPROG complexes (+) in pure water. For all complexes, Cy5-plasmid DNA was used for labeling. The mean dwell times of both DNA/bPEI and COPROG complexes indicates comparable complex sizes.

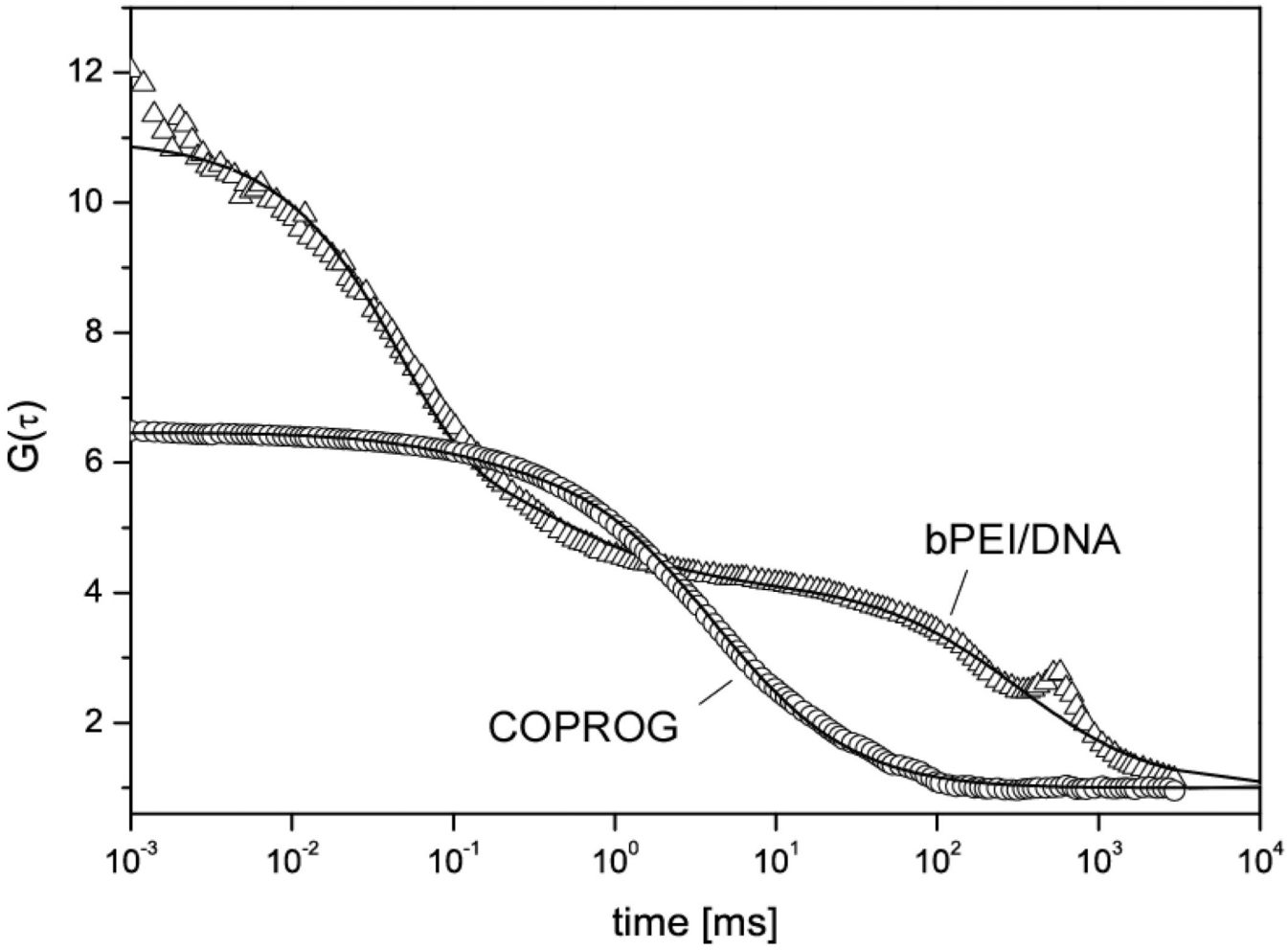

Figure 3.
FCS autocorrelation curves of bPEI/DNA (Δ) and COPROG complexes (○) in 150 mM NaCl. For all complexes, Cy5-plasmid DNA was used for labeling. The measurements in physiological salt solution show a great difference in size and polydispersity of the particles. COPROG complexes maintain similar particle size as in pure water. bPEI/DNA complexes aggregate severely.

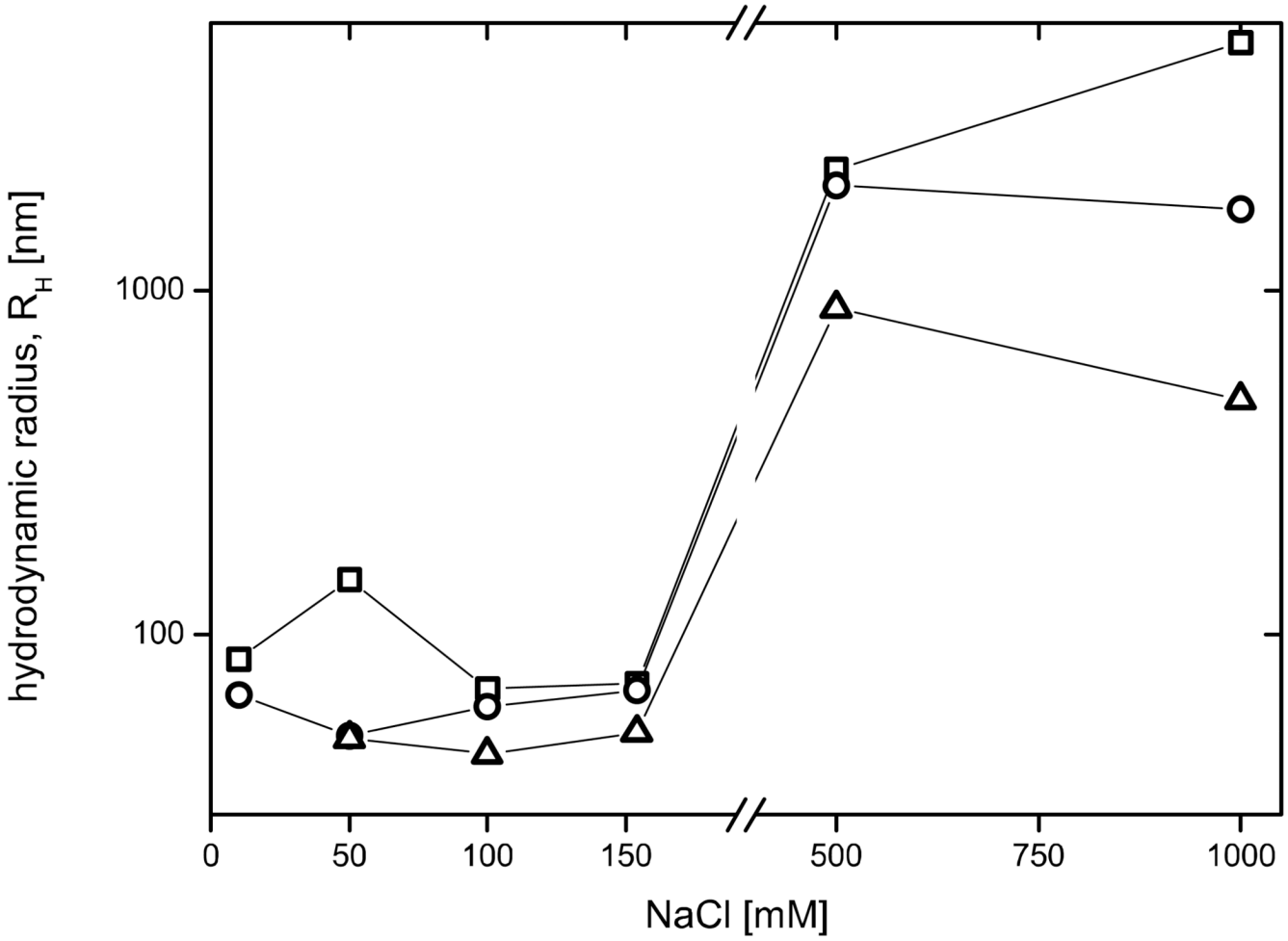

Figure 4.

Variation of the hydrodynamic radii (R_H) of COPROGs mixed at N/P ratios of 8 (□), 10 (○) and 12 (Δ) with a constant three charge equivalents of P6YE5C in solution as a function of external NaCl concentration. COPROG complexes for all three formulations maintain stability at low to physiological salt concentrations. At higher NaCl concentrations, the COPROGs start to aggregate.

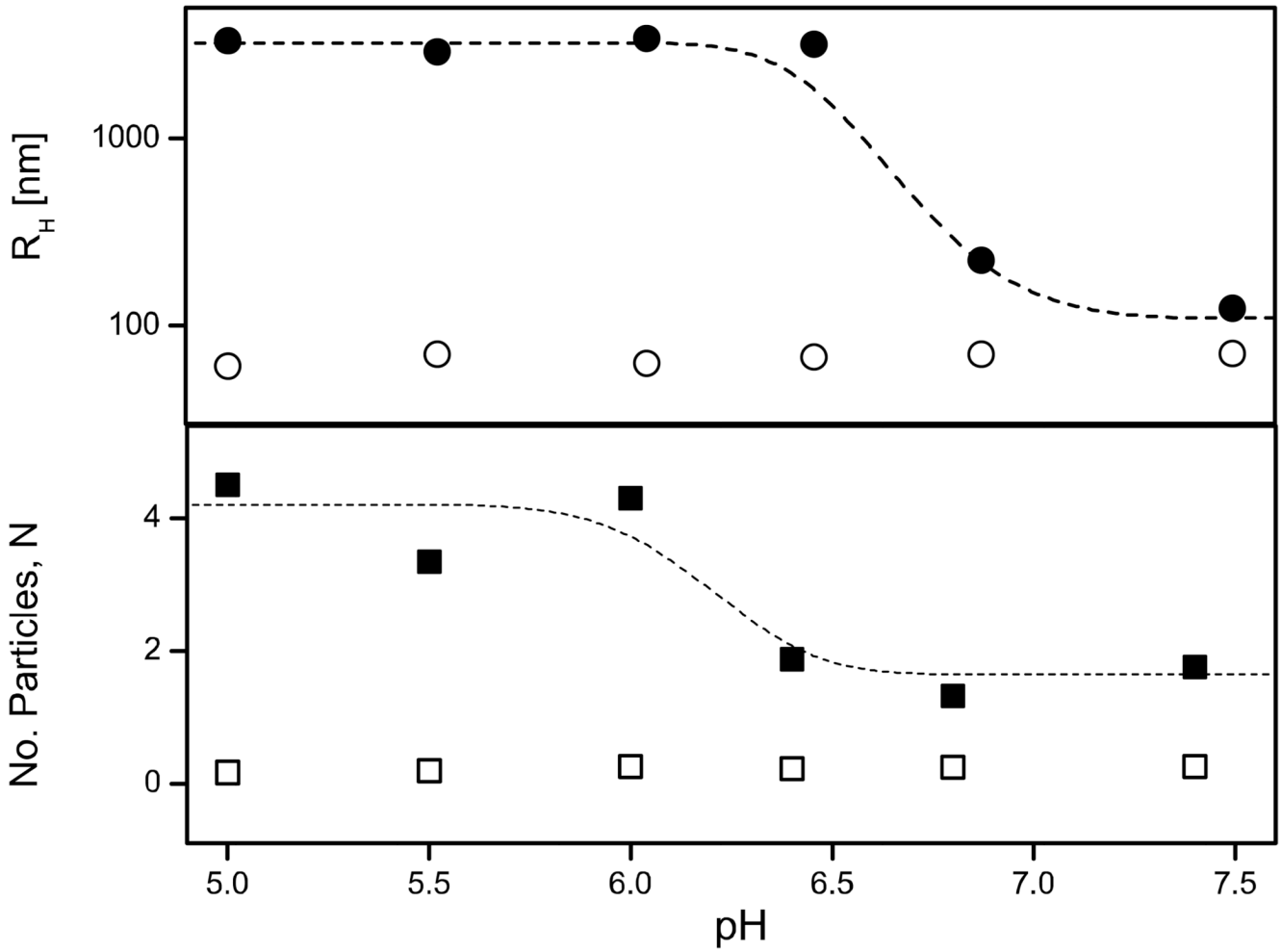

Figure 5.

Hydrodynamic radii, R_H and total number of particles, N for DNA/bPEI (N/P = 8) [filled] and COPROG (N/P = 8, 3 charge equivalent P6YE5C) [open] complexes at pH values ranging from 5 to 7.4 from FCS measurements. For all complexes, Alexa488-bPEI was used for labeling. COPROG complexes are highly stable to pH with no influence on the stability or number of the COPROG complexes. bPEI polyplexes are seen to aggregate at low pH resulting in a large increase in the apparent RH. The total number of particles N, however, also increased approximately two fold suggesting the amount of unbound bPEI increased at low pH.

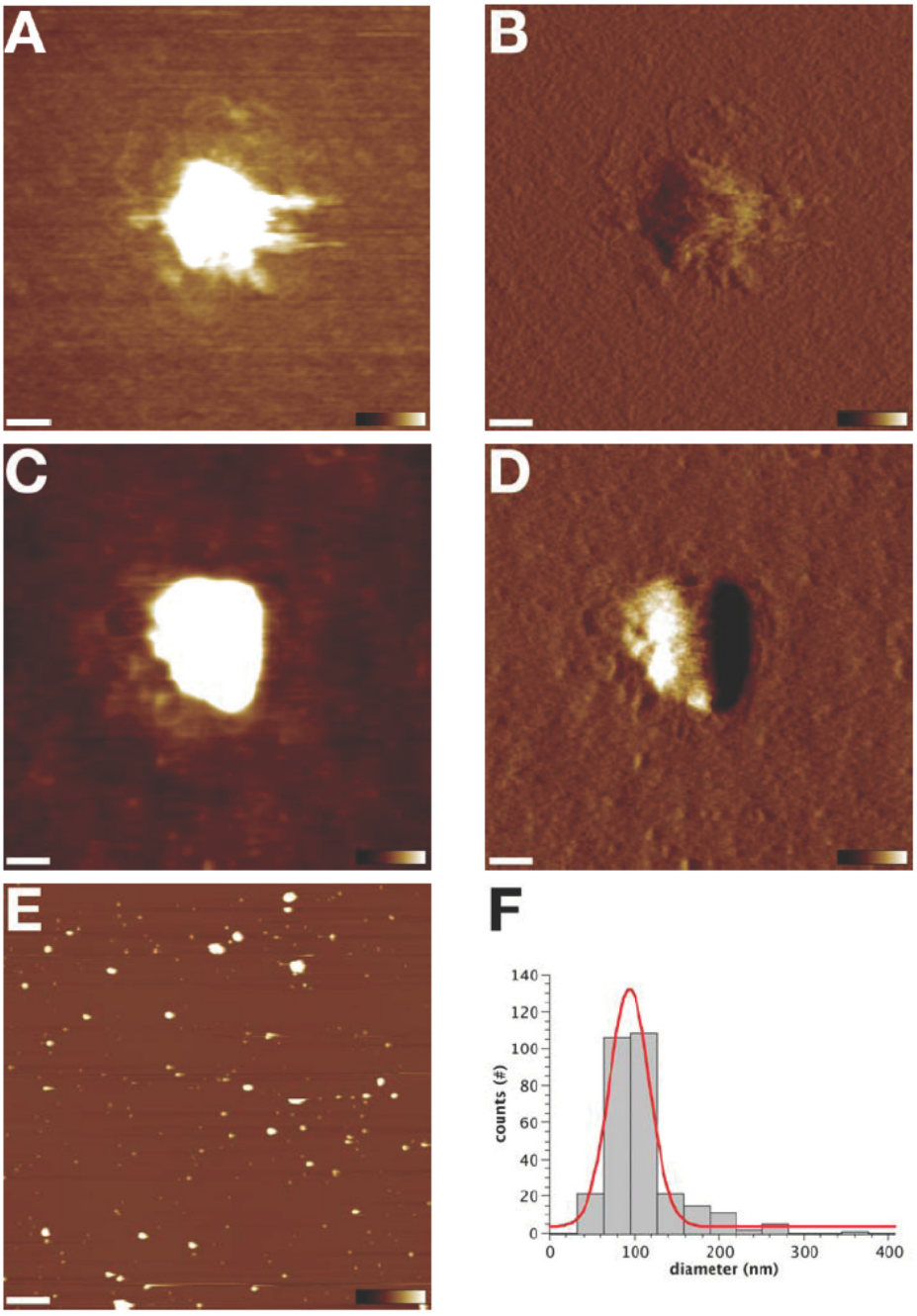

Figure 6.

AFM height (A) and amplitude image (B) of one bPEI/DNA complex (N/P 8) on a freshly cleaved untreated mica surface imaged in ultrapure water. Due to the excess free polycations, bPEI/DNA particles adhere consistently to the untreated negatively charged mica surfaces. AFM height (C) and amplitude image (D) of one COPROG complex on a freshly cleaved TAE/Mg^{2+} treated mica surface imaged in ultrapure water. COPROGs adhere consistently on Mg-treated mica surfaces. All images (A–D) are 500 × 500 nm with 50 nm scale bars. Height scale is 4 nm and 50 mV for height and amplitude images respectively. By scanning a larger area (10 μm, 100 nm height) as shown in (F) the size

distribution of the COPROGs was calculated and a Gaussian fit to the distribution gives a mean diameter of 94.2 nm ± 23.5 nm in good agreement with FCS measurements.

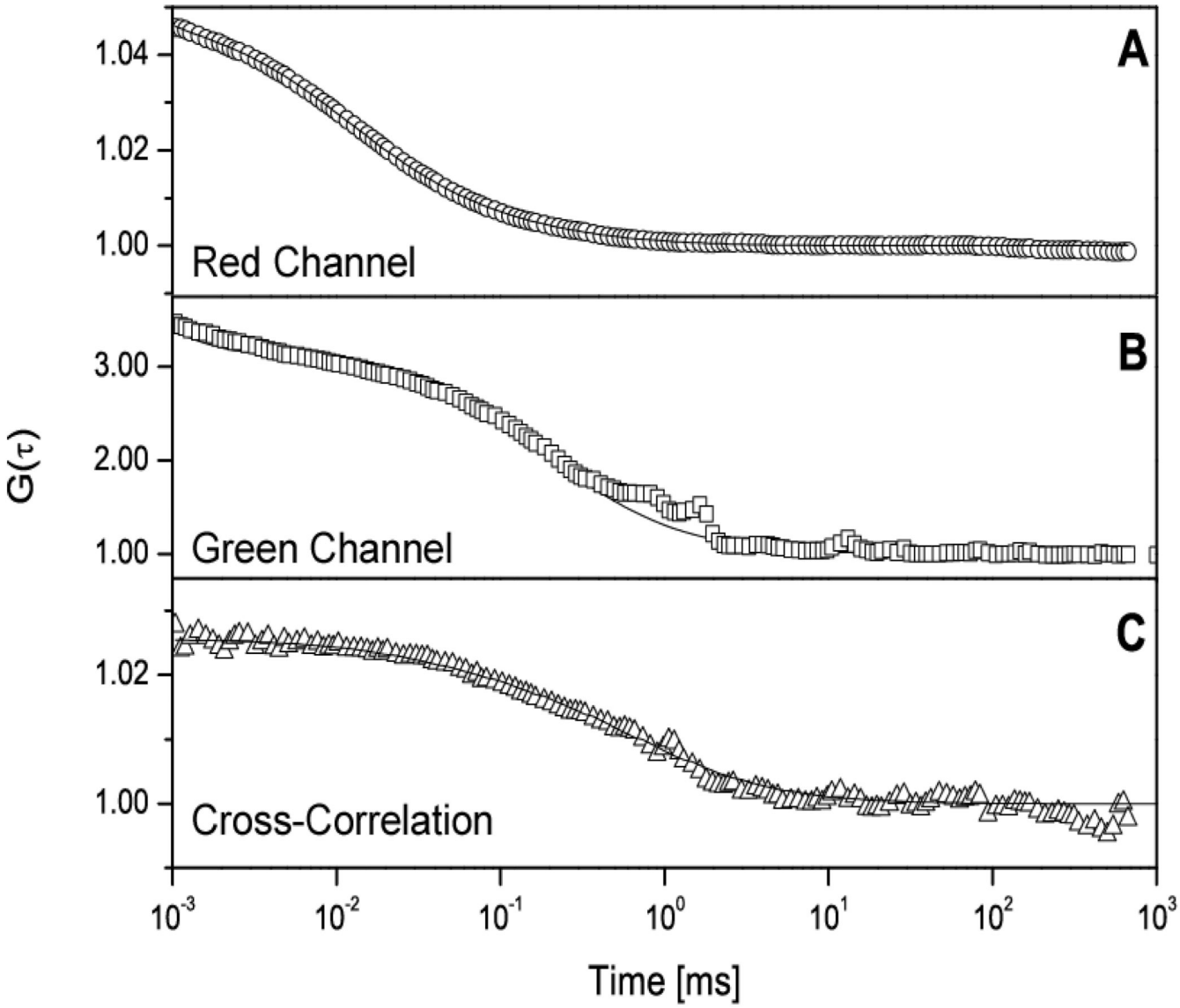

Figure 7.
Dual-color fluorescence cross-correlation spectroscopy (FCCS) autocorrelations (7A, red channel; 7B green channel) curves and resulting cross-correlation (C) from COPROG complexes with Alexa488 labeled bPEI and Alexa 633 labeled P6YE5C. All curves are well described by a two-component fit. Solid lines represent best fits.

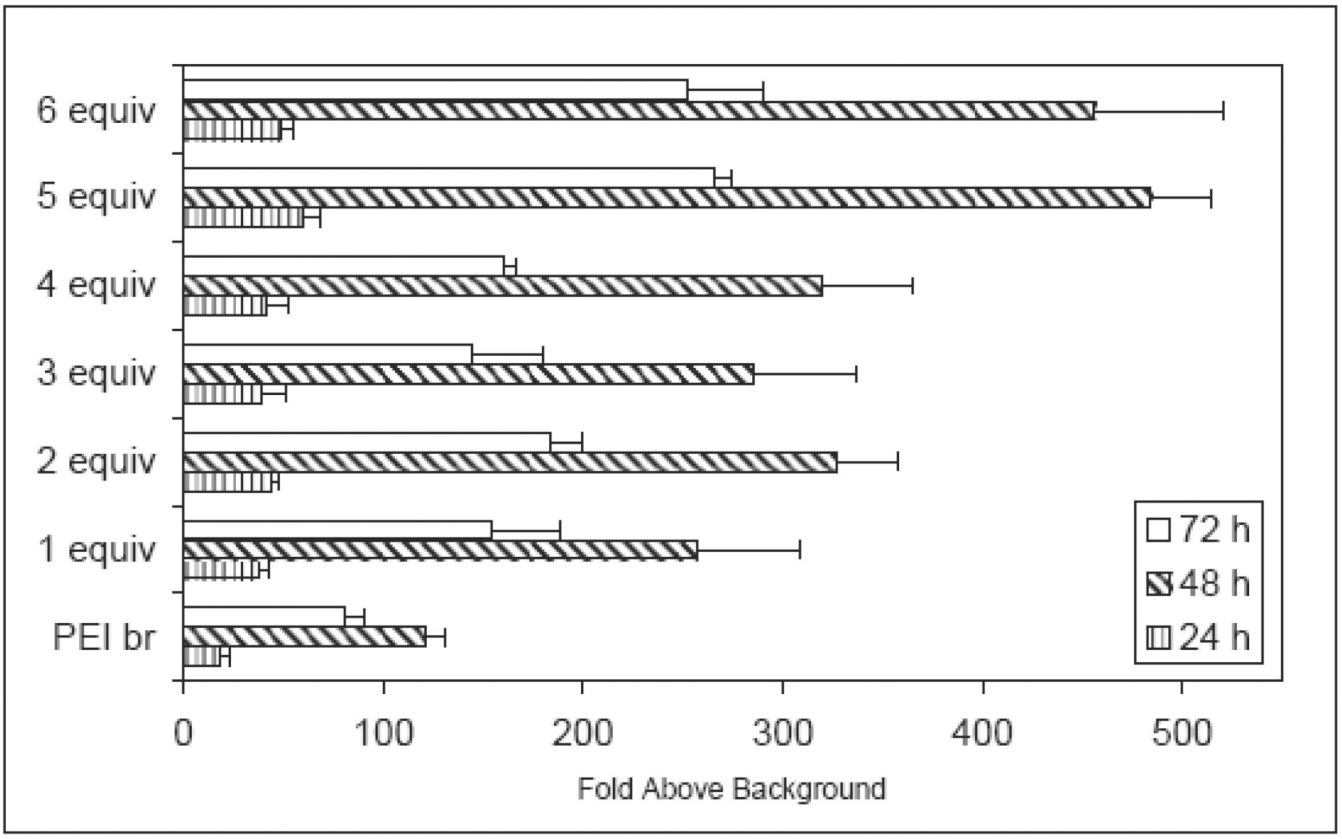

Figure 8.

Comparative transfection efficiencies of bPEI/DNA and COPROG complexes in NIH 3T3 cells. Transfection efficiencies were measured after 24, 48 and 72 hours with a Metridias Luciferase assay. The efficiencies of the COPROGs were investigated for 6 different concentrations of copolymer equivalents. All COPROG formulations showed a two to four fold increase in reporter gene expression compared to bPEI/DNA.

Table 1

Single-color-FCS measurements of Alexa488 labeled bPEI and Alexa633 labeled P6YE5C polymer.

Component	Channel	τ_D (μs)	D (m^2s^{-1})
bPEI	green	30	2.6×10^{-10}
P6YE5C	red	124	6.0×10^{-11}

Table 2

Dual-color-FCCS results. Dwell times and percentages of the slow and fast fraction from the fits.

Channel	τ_{D1} (ms)	fast fraction ρ_1 (%)	τ_{D2} (ms)	slow fraction ρ_2 (%)
Red	0.124	93.6	3.319	6.4
Green	0.155	25.8	3.289	74.4
Cross-Correlation	0.155	17.8	5.360	82.2

Table 3

Distribution percentages of bPEI and P6YE5C among the components of the COPROG system.

	Free bPEI	Free P6YE5C	bPEI- P6YE5C	COPROG
bPEI	0	-	25	75
P6YE5C	-	70	23.4	6.5